Available online at www.sciencedirect.com
ScienceDirect
International Journal for Parasitology 38 (2008) 839–850
www.elsevier.com/locate/ijpara

Genetic profiling of *Trypanosoma cruzi* directly in infected tissues using nested PCR of polymorphic microsatellites

Helder Magno Silva Valadares [a,1], Juliana Ramos Pimenta [a,1], Jorge Marcelo de Freitas [a], Tomás Duffy [b], Daniella C. Bartholomeu [c], Riva de Paula Oliveira [d], Egler Chiari [c], Maria da Consolação Vieira Moreira [e], Geraldo Brasileiro Filho [f], Alejandro Gabriel Schijman [b], Glória Regina Franco [a], Carlos Renato Machado [a], Sérgio Danilo Junho Pena [a], Andréa Mara Macedo [a,*]

[a] *Departamento de Bioquímica e Imunologia, Instituto de Ciências Biológicas, Universidade Federal de Minas Gerais, Av. Antônio Carlos 6627, Caixa Postal 486, 30161970 Belo Horizonte, MG, Brazil*
[b] *Laboratorio de Biología Molecular de la Enfermedad de Chagas, Instituto de Investigaciones en Ingeniería Genética y Biología Molecular (INGEBI-CONICET), Buenos Aires, Argentina*
[c] *Departamento de Parasitologia, Instituto de Ciências Biológicas, Universidade Federal de Minas Gerais, Brazil*
[d] *Joslin Diabetes Center, Section in Developmental and Stem Cell Biology, Boston, MA, United States*
[e] *Departamento de Clínica Médica, Faculdade de Medicina, Universidade Federal de Minas Gerais, Brazil*
[f] *Departamento de Anatomia Patológica e Medicina Legal, Faculdade de Medicina, Universidade Federal de Minas Gerais, Brazil*

Received 1 August 2007; received in revised form 15 October 2007; accepted 25 October 2007

Abstract

The investigation of the importance of the genetics of *Trypanosoma cruzi* in determining the clinical course of Chagas disease will depend on precise characterisation of the parasites present in the tissue lesions. This can be adequately accomplished by the use of hypervariable nuclear markers such as microsatellites. However the unilocal nature of these loci and the scarcity of parasites in chronic lesions make it necessary to use high sensitivity PCR with nested primers, whose design depends on the availability of long flanking regions, a feature not hitherto available for any known *T. cruzi* microsatellites. Herein, making use of the extensive *T. cruzi* genome sequence now available and using the Tandem Repeats Finder software, it was possible to identify and characterise seven new microsatellite loci – six composed of trinucleotide (TcTAC15, TcTAT20, TcAAT8, TcATT14, TcGAG10 and TcCAA10) and one composed of tetranucleotide (TcAAAT6) motifs. All except the TcCAA10 locus were physically mapped onto distinct intergenic regions of chromosome III of the CL Brener clone contigs. The TcCAA10 locus was localised within a hypothetical protein gene in the *T. cruzi* genome. All microsatellites were polymorphic and useful for *T. cruzi* genetic variability studies. Using the TcTAC15 locus it was possible to separate the strains belonging to the *T. cruzi* I lineage (DTU I) from those belonging to *T. cruzi* II (DTU IIb), *T. cruzi* III (DTU IIc) and a hybrid group (DTU IId, IIe). The long flanking regions of these novel microsatellites allowed construction of nested primers and the use of full nested PCR protocols. This strategy enabled us to detect and differentiate *T. cruzi* strains directly in clinical specimens including heart, blood, CSF and skin tissues from patients in the acute and chronic phases of Chagas disease.

Keywords: *Trypanosoma cruzi*; Chagas disease; Genome project; Polymorphic microsatellites; Full nested PCR

1. Introduction

The clinical features of Chagas disease, an American parasitic disease caused by *Trypanosoma cruzi*, are quite variable, ranging from asymptomatic cases to severe

* Corresponding author. Tel.: +55 31 34992641; fax: +55 31 34992984.
E-mail address: andrea@icb.ufmg.br (A.M. Macedo).
[1] Both authors contributed equally to the work.

0020-7519/$34.00
doi:10.1016/j.ijpara.2007.10.017

chronic cardiovascular and/or gastrointestinal involvement. This pleiotropy results from a complex interaction between environmental and genetic factors associated with both the host and parasite (Macedo and Pena, 1998; Macedo et al., 2004).

Although the first draft of the *T. cruzi* genome sequence has already been published (El-Sayed et al., 2005), most aspects of its population structure and evolution remain to be elucidated. Since 1999, a clear division of the parasite into two major evolutionary lineages presenting a high phylogenetic divergence and distinct epidemiological characteristics has been recognised and named *T. cruzi* I and *T. cruzi* II, the latter being much more associated with chronic cases of the disease, at least in the southern cone of Latin America (Souto et al., 1996; Zingales et al., 1998; Momen, 1999; Di Noia et al., 2002; Burgos et al., 2005; Freitas et al., 2005). Nevertheless, cases of human infection by *T. cruzi* I associated with severe symptoms of Chagas disease have been found, especially in the northern part of South America (Coura et al., 2002; Añez et al., 2004; Teixeira et al., 2006). We recently characterised a third ancestral lineage, called *T. cruzi* III (Freitas et al., 2006). Within the three major evolutionary lineages there is substantial genetic and phenotypic diversity that has been unravelled with polymorphic markers such as isoenzymes, random amplified polymorphic DNA (RAPD), minisatellites, microsatellites and others (Miles et al., 1978; Romanha et al., 1979; Tibayrenc et al., 1986; Macedo et al., 1992; Oliveira et al., 1998; Brisse et al., 2000, 2001; Macedo et al., 2001, 2004).

To date, no correlation between the genetic variability of the parasite and the clinical characteristics of the disease was clearly demonstrated (Macedo and Pena, 1998; Zingales et al., 1999). This can be explained, at least in part, by the fact that *T. cruzi* strains are multiclonal populations presenting differential tissue tropisms (Melo and Brener, 1978; Morel et al., 1980; Andrade, 1985; Tibayrenc et al., 1986; Macedo et al., 1992; Oliveira et al., 1998; Andrade et al., 1999). Thus, parasites isolated from patients' blood, maintained in laboratory conditions and available for analyses, can differ from those directly involved in the tissue lesions which probably have a stronger association with the disease symptoms (Macedo and Pena, 1998).

To characterise *T. cruzi* directly in infected tissues a technique is required that is sensitive enough to distinguish between individual clones and to detect small amounts of parasite DNA present in the biological samples. In this context, the advent of low-stringency single-specific primer (LSSP)-PCR has offered new possibilities in the epidemiological studies of the *T. cruzi* infection, demonstrating the existence of differential tissue homing for distinct parasites both in human and in experimental infections, and the strict association between the presence of the parasite and the tissue injury (Macedo and Pena, 1998; Vago et al., 2000; Burgos et al., 2005). The LSSP-PCR technique, however, presents some limitations. Firstly, the target of LSSP-PCR was DNA variation in the minicircles and not in the nuclear genome, where the most important evolutionary phenomena probably take place. Also, the high complexity and the multilocal nature of LSSP-PCR do not offer a simple way to determine the number and the composition of parasites present in a specific sample.

In an effort to overcome the limitations of LSSP-PCR, we recently described (Freitas et al., 2005) the successful application of a real-time hemi-nested PCR strategy for amplifying 24Sα rDNA alleles directly from infected human tissues. We were able to report the predominance of *T. cruzi* type II parasites in heart, oesophageal and colon samples from Brazilian patients (Freitas et al., 2005). However, rDNA is a conserved marker and therefore inadequate for distinguishing strains and clones within the major lineages. Another strategy initially described by Veas et al. (1991) and used to evaluate *T. cruzi* genetic diversity consists of the amplification of the parasite kinetoplast-DNA (kDNA) followed by hybridization of amplicons with labelled hypevariable kDNA domains for each particular lineage. By means of this technique Virreira et al. (2006) were able to discriminate the *T. cruzi* sublineages directly in megacolon samples of Bolivian patients. However, similar to 24Sα rDNA, this technique did not allow the differentiation of strains and clones within the major lineages.

Microsatellites, on the other hand, are hypervariable nuclear markers that, when multiplexed, render highly individual and reproducible profiles (Oliveira et al., 1998; Macedo et al., 2001, 2004). They have the drawback of being single copy DNA sequences, making PCR amplification from the very small amounts of parasite DNA present in chronically infected tissues a difficult task. This limitation can be solved by use of the exquisitely sensitive strategy of nested PCR. The problem is that the *T. cruzi* microsatellite loci available thus far are $(CA)_n$ repeats with short flanking regions obtained by affinity capture using probes attached to streptavidin-coated magnetic beads (Oliveira et al., 1998). For the design of nested primers we need long flanking regions.

In the present work, we made use of the extensive *T. cruzi* genome sequence now available and used the Tandem Repeats Finder programme to identify microsatellite loci with tri- and tetranucleotide repeat motifs, with longer flanking regions. Application of nested PCR to these microsatellite loci allowed us to obtain genetic profiles of *T. cruzi* directly in infected human and animal tissues.

2. Materials and methods

2.1. Microsatellite loci identification

Four DNA sequences derived from the sequencing of chromosome III of the *T. cruzi* CL Brener clone (Andersson et al., 1998) (Accession Nos. AC137988, AF05831, AF05832 and AF05833) and two DNA sequences from unknown chromosomes (Accession Nos. BH842909.1 and

AC096913.1) were retrieved from Genbank and submitted to the Tandem Repeats Finder programme (Benson, 1999).

2.2. Physical mapping of microsatellite loci

The microsatellite loci and the corresponding flanking regions were mapped on the CL Brener annotated genome (El-Sayed et al., 2005), using the Basic Local Alignment Search Tool (BLAST) algorithm.

2.3. Parasites

The *T. cruzi* DNA samples used in this study were obtained by two of the authors (Egler Chiari and Alejandro Gabriel Schijman) or kindly provided by Dr. Octávio Fernandes and Dr. José Rodrigues Coura, Departamento de Medicina Tropical, Fiocruz, Rio de Janeiro; Dr. Bianca Zingales, Universidade de São Paulo, Brazil; Dr. M. Tibayrenc from the Centre d'Etudes sur le Polymorphisme des Microorganismes, Montpellier, France; and Dr. Stella Gonzalez Cappa, Facultad de Medicina, Universidad de Buenos Aires, Argentina (Table 1).

2.4. Mouse tissue samples

Heart and rectum were obtained from three inbred male mice (BALB/C) infected with 50 trypomastigotes of the JG strain plus 50 trypomastigotes of the Col 1.7G2 clone (clone obtained by serial dilution from the Colombiana strain, which belongs to the *T. cruzi* I lineage) and sacrificed after 6 months of infection. Tissue samples were processed by alkaline lysis with 50 mM NaOH followed by neutralisation with 130 mM Tris–HCl pH 7.0 and 3 μL were used directly in a PCR reaction after 10-fold dilution in sterile water (Andrade et al., 1999). Tissues samples of non-infected mice were also used as negative controls in the PCR assays. All animal procedures were performed in accordance with the Code of Ethical Conduct.

2.5. Human tissue samples

We analysed heart tissue fragments (left ventricle) obtained from two patients with chronic chagasic cardiopathy and severe congestive cardiac failure, without digestive megasyndromes. Samples labelled JP and DF were

Table 1
Characteristics of *Trypanosoma cruzi* strains analysed

Strain	Host/Vector	Origin	DTU[a]	Major lineage[b]
1009	*Panstrongilus megistus*	MG/Brazil	I	*T. cruzi* I
Col18/5	*Homo sapiens*	Colombia	I	*T. cruzi* I
ColRS	*Homo sapiens*	Colombia	I	*T. cruzi* I
D7	*Didelphis marsupialis*	RJ/ Brazil	I	*T. cruzi* I
K98[c]	*Homo sapiens*	Argentine	I	*T. cruzi* I
RB1	*Rhodnius brethesi*	AM/ Brazil	I	*T. cruzi* I
84	*Homo sapiens*	MG/Brazil	IIb	*T. cruzi* II
209	*Homo sapiens*	MG/Brazil	IIb	*T. cruzi* II
578	*Homo sapiens*	GO/Brazil	IIb	*T. cruzi* II
580	*Homo sapiens*	GO/Brazil	IIb	*T. cruzi* II
581	*Homo sapiens*	GO/Brazil	IIb	*T. cruzi* II
1014	*Panstrongilus megistus*	MG/Brazil	IIb	*T. cruzi* II
1043	*Homo sapiens*	MG/Brazil	IIb	*T. cruzi* II
200pm	*Homo sapiens*	MG/Brazil	IIb	*T. cruzi* II
Bas	*Homo sapiens*	MG/Brazil	IIb	*T. cruzi* II
CPI11/94	*Homo sapiens*	PI/ Brazil	IIb	*T. cruzi* II
CPI94/95	*Homo sapiens*	PI/ Brazil	IIb	*T. cruzi* II
GLT564	*Leonthopitecus rosalia*	RJ/ Brazil	IIb	*T. cruzi* II
GOCH	*Homo sapiens*	MG/Brazil	IIb	*T. cruzi* II
JG	*Homo sapiens*	MG/Brazil	IIb	*T. cruzi* II
MCS156949	*Homo sapiens*	DF/ Brazil	IIb	*T. cruzi* II
MPD	*Homo sapiens*	MG/Brazil	IIb	*T. cruzi* II
231	*Homo sapiens*	MG/Brazil	IIc	*T. cruzi* III
226	*Homo sapiens*	MG/Brazil	IIc	*T. cruzi* III
3869	*Homo sapiens*	AM/Brazil	IIc	*T. cruzi* III
4182	*Rhodnius brethesi*	AM/Brazil	IIc	*T. cruzi* III
182	*Homo sapiens*	MG/Brazil	IId/e	Hybrid
CL Brener	*Triatoma infestans*	MG/Brazil	IIe	Hybrid
RA[c]	*Homo sapiens*	Argentine	IId/e	Hybrid
SO3 cl5	*Triatoma infestans*	Bolivia	IId	Hybrid
CanIII	*Homo sapiens*	PA/Brazil	IIa	N.D[d]

[a] DTUs I, IIa, IIb, IIc, IId and IIe are classifications for *T. cruzi* strains described by Brisse et al. (2000, 2001).
[b] Abbreviations for the major lineages of *T. cruzi* in accordance with Freitas et al. (2006) are *T. cruzi* I, *T. cruzi* II and *T. cruzi* III.
[c] The lineage of *T. cruzi* strains was previously determined by amplification of the rDNA24Sα gene (Souto et al., 1996) and Citocrome Oxidase II *Alu*I restriction fragment length polymorphism (Freitas et al., 2006).
[d] N.D., not determined.

obtained from hearts removed from patients during cardiac transplants at the Surgical Center of the Hospital Felicio Rocho, Belo Horizonte, MG, Brazil. Tissue samples were processed using an alkaline lysis protocol as described above. We also analysed clinical samples from infected Argentinean patients, namely blood from two patients with severe chronic Chagas heart disease (ChHD-S and ChHD-T), blood and CSF samples from a patient with Chagas encephalytis (AS and AL, respectively), blood from a neonate with Congenital Chagas disease (HE), placental tissue from a pregnant woman (Pl) and a skin biopsy from an epidermic chagoma from a patient with Chagas reactivation due to a heart transplant (Sk-L). Blood samples were conserved in guanidine-HCL pH 8.0 solution and 200 μL of this material was submitted to total DNA extraction with phenol:chloroform:isoamyl alcohol (25:24:1). The total DNA was precipitated using 10% sodium acetate 3 M and absolute ethanol. The DNA was then suspended in 20 μL of sterile water and 3 μL were used for PCR assays. Alternatively, DNA from some human tissue samples was obtained using the QiAmp tissue kit (Qiagen, CA, USA) as previously described (Schijman et al., 2000). This study fulfilled all criteria required by the Medical Code of Ethics and the Helsinki II statement and was approved by two independent Ethical Committees from Universidade Federal de Minas Gerais, Belo Horizonte, Brazil and INGEBI-CONICET, Buenos Aires, Argentina. Informed consents were obtained from the patients or their families.

2.6. Microsatellite PCR assay

Two pairs of primers flanking each microsatellite locus (TcTAT20, TcAAT8, TcTAC15, TcGAG10, TcCAA10, TcATT14 and TcAAAT6) were designed using the Oligo version 4.0 programme (Rychlick, 1992). We added the suffix ex to the external primer nomenclatures and to differentiate those from internal primers (Table 2). To analyse the polymorphism of these loci into different *T. cruzi* strains, each PCR was performed in a total volume of 15 μL containing 10 mM Tris–HCl pH 9.0, 50 mM KCl, 0.1% Triton X-100 (Buffer B, Promega, Madison, Wiscosin, USA), 2.5 mM $MgCl_2$ (Promega), 0.5 U Taq DNA Polymerase (Promega), 250 μM of each dNTP, 0.3 μM of each primer (only internal reverse and forward primers) and 3 μL of DNA template (1 ng/μL) recovered with mineral oil. Amplification was performed in a PT100 thermocycler (MJ Research) using the step-down protocol (Hecker and Roux, 1996) modified for amplification of *T. cruzi* DNA: an initial denaturation step at 94 °C for 5 min; annealing at 58 °C for 30 s; primer extension at 72 °C for 1 min and a denaturation step at 94 °C for 30 s. After every five cycles, the annealing temperature was decreased to 55, 53, 51 and 48 °C. At this last temperature, the number of cycles was increased to 15, followed by a final extension step at 72 °C for 10 min. To amplify small amounts of parasite DNA, such as those found in chronically infected tissues, a full nested PCR protocol was applied: the first round used the external pair of primers followed by a second round employing the internal pair. For both rounds, we used the same PCR conditions described above. For the second PCR round, 10% of the amplified products obtained in the first PCR round were used as a DNA template.

Table 2
Sequence of primers designed to amplify the *Trypanosoma cruzi* microsatellite loci TcAAT8, TcATT14, TcCAA10, TcGAG10, TcTAC15, TcTAT20 and TcAAAT6

Primer	Sequence
TcAAT8-forward	5′-FluresceinACCTCATCGGTGTGC ATGTC-3′
TcAAT8-reverse	5′-TATTGTCGCCGTGCAATTTC-3′
TcAAT8ex-forward	5′-AGAGGCGCACAGTTGTATGC-3′
TcAAT8ex-reverse	5′-GACGCTTTATGTTGAATTCA-3′
TcATT14-forward	5′-FluresceinTTATGGATGGGGTGGGT TTG-3′
TcATT14-reverse	5′-AGCAATAATCGTATTACGGC-3′
TcATT14ex-forward	5′-TTTGCAAATGGGACAGTTAC-3′
TcATT14ex-reverse	5′-ACCTATTTTGCTCCTTGGTG-3′
TcCAA10-forward	5′-FluresceinGCACAGGGAGTCAAACT TCA-3′
TcCAA10-reverse	5′-TCAAATTTATCACCCGTCGA-3′
TcCAA10ex-forward	5′-GGTAAGGGCGAGTATGACTG-3′
TcCAA10ex-reverse	5′-TAGCCAATAAAAGTGATGCC-3′
TcGAG10-forward	5′-FluresceinTTCTCGGCTTCTATGTG TGC-3′
TcGAG10-reverse	5′-GTGCCCTCCGTTTATTCCTC-3′
TcGAG10ex-forward	5′-TTTCTTACTGCGAGGTGAGT-3′
TcGAG10ex-reverse	5′-AAGTGAAGTGAAGTGGTGCC-3′
TcTAC15-forward	5′-FluresceinGAATTTCCCCATTTCCA AGC-3′
TcTAC15-reverse	5′-CGATGAGCAACAATCGCTTC-3′
TcTAC15ex-forward	5′-GGATATTTGTTACTGCTGGC-3′
TcTAC15ex-reverse	5′-CGGACATATCCCTCTAGTCG-3′
TcTAT20-forward	5′-FluresceinGATCCTTGAGCAGCCAC CAA-3′
TcTAT20-reverse	5′-CAAATTCCCAACGCAGCAGC-3′
TcTAT20ex-forward	5′-AGGCTGATCCTTGAGCAGCC-3′
TcTAT20ex-reverse	5′-CGGCGGTCTTCTTTTGTCTC-3′
TcAAAT6-forward	5′-FluresceinGCCGTGTCCTAAAGA GCAAG-3′
TcAAAT6-reverse	5′-GGTTTTAGGGCCTTTAGGTG-3′
TcAAAT6ex-forward	5′-ACGCACTCTCTTTGTTAACAG-3′
TcAAAT6ex-reverse	5′-CACATACACATTCCAATGGTT-3′

2.7. Allele sizes

To determinate the allele sizes, 1–3 μl of the PCR fluorescent products were analysed in a 6% denaturing polyacrylamide gel of an automatic laser fluorescent (ALF) sequencer (GE Healthcare, Milwaukee, Wisconsin, USA) and comparised with fluorescent DNA fragments of 50–500 bp using Allelelocator software (GE Healthcare).

2.8. Statistical parameters

The expected and observed heterozygosis for each locus and the linkage disequilibrium between those were calculated using the Arlequin 2.0 programme.

2.9. LSSP-PCR

This technique was performed according to Andrade et al. (1999).

3. Results

3.1. Microsatellite loci identification and characterisation

Tandem Repeats Finder analyses of *T. cruzi* DNA sequences detected 36 microsatellite loci with different repeat motifs (seven mono-, eleven di-, eight tri-, two tetra-, three penta- and five hexanucleotides), from which seven were selected and characterised: the $(AAT)_8$ and $(AAAT)_6$ loci from AF052831, $(TAT)_{20}$ locus from AF052832, $(TAC)_{15}$ locus from AF052833, $(GAG)_{10}$ locus from AC137988, $(ATT)_{14}$ locus from AC096913.1 and $(CAA)_{10}$ locus from BH842909.1, which were named TcAAT8, TcAAAT6, TcTAT20, TcTAC15, TcGAG10, TcATT14 and TcCAA10, respectively. These loci were specifically selected based on the length of the repetition motifs (tri- and tetranucleotides) and the absence of interruptions within those, which provide a high degree of polymorphism and stability in laboratory amplifications.

The analysis of 31 *T. cruzi* strains showed that all seven microsatellite loci were polymorphic. TcAAT8 was the microsatellite locus with the greatest number of alleles (14 alleles of different sizes ranging from 229 to 298 bp), followed by TcTAT20 (13 alleles from 175 to 238 bp), TcTAC15 (nine alleles between 96 and 144 bp), TcCAA10 (eight alleles from 125 to 161 bp), TcATT14 and TcAAAT6 (seven alleles with 253 to 274 and 255 to 279 bp, respectively). TcGAG10 was the locus with the lowest number of alleles (six alleles from 129 to 144 bp) (Table 3). The 99 bp alleles for the locus TcTAC15 was found in all analysed *T. cruzi* II strains and in some of the *T. cruzi* III and hybrid strains, but not in *T. cruzi* I. In the *T. cruzi* I strain, only the allele of 96 bp was amplified (Table 3). We tested 10 additional strains and/or clones belonging to the *T. cruzi* I lineage (Dm28c, D11, G, Gambá

Table 3
Allele sizes in bp obtained for each of the seven loci analysed in 31 *Trypanosoma cruzi* strains

Loci	TcAAAT6	TcAAT8	TcTAT20	TcTAC15	TcATT14	TcGAG10	TcCAA10
T. cruzi I strains							
1009	263/263	250/250	190/208	96/96	253/256	141/141	143/146
Col18/5	255/255	229/229	181/181	96/96	253/253	144/144	125/125
ColRS	255/255	229/229	181/181	96/96	253/253	144/144	125/125
D7	255/255	244/244	235/235	96/96	253/253	144/144	125/125
K98	255/255	N.A.[a]	178/178	96/96	253/253	144/144	N.A.[a]
RBI	255/259	229/229	184/184	96/96	256/256	141/144	N.A.[a]
T. cruzi II strains							
84	271/275	259/298	190/190	99/99	262/262	129/129	152/152
209	263/271	253/298	208/214	99/99	265/265	129/129	143/146
578	271/275	262/298	214/238	99/99	262/262	129/129	146/155
580	263/275	253/262	190/238	99/99	265/265	129/144	143/155
581	271/275	262/298	214/238	99/99	262/262	129/129	146/155
1014	271/271	259/259	205/217	99/99	265/265	141/141	146/155
1043	263/267	250/253	211/223	99/99	253/268	129/144	146/161
200pm	263/275	253/298	205/208	99/99	262/262	129/135	146/152
Bas	271/275	259/268	190/196	99/99	265/265	144/144	146/155
CPI11/94	263/275	250/259	190/205	99/99	253/265	132/144	146/155
CPI94/95	263/275	250/250	190/205	99/99	253/265	135/144	146/146
GLT564	275/275	247/262	208/208	99/99	265/265	144/144	155/158
GOCH	263/275	250/259	190/205	99/99	253/262	129/144	146/155
JG	271/275	262/262	190/217	99/99	265/265	141/144	143/146
MCS156949	275/275	259/268	190/205	99/99	262/262	129/144	146/152
MPD	275/275	244/244	214/214	99/99	265/265	135/141	152/155
T. cruzi III strains							
226	263/271	292/295	184/208	99/99	256/265	129/138	131/143
231	267/279	292/295	184/184	120/141	256/256	138/144	143/143
3869	267/267	295/295	181/181	129/144	256/256	138/144	143/143
4182	275/279	292/295	181/181	132/141	262/274	138/138	131/131
T. cruzi hybrid and/or misclassified strains							
182	267/279	292/295	184/184	120/129	253/265	138/138	131/131
CL Brener	263/263	247/292	181/223	129/141	265/271	144/144	131/155
RA	263/263	247/247	181/223	129/129	265/271	144/144	155/155
SO3	259/271	250/292	184/220	99/135	265/265	144/144	152/152
CanIII	271/271	277/280	175/175	105/105	253/268	138/138	131/131

[a] N.A., not amplified by PCR.

cl1, Ops21 cl11, P209 cl1, Silvio X10 cl1, RBI, RBVI, RBVII), which confirmed that the 96 bp allele is characteristic of this lineage (data not shown).

As previously demonstrated (Oliveira et al., 1998), a significant divergence between the observed and expected heterozygosis, indicating great departure from the Hardy–Weinberg equilibrium, was verified for all analysed loci. Furthermore, a high degree of linkage disequilibrium was found in all possible pair-wise combinations of the seven loci analysed. The χ^2 values ranged from 38.3 to 150.6 and all were significant at $P < 0.05$ (data not shown).

3.2. Physical mapping of microsatellite loci

Based on genomic (El-Sayed et al., 2005) and karyotype (Branche et al., 2006) data, we were able to map the microsatellite loci TcAAT8, TcAAAT6, TcTAT20, TcTAC15, TcGAG10 and TcATT14 onto the scaffolds 1047053516941 (non-Esmeraldo-like haplotype) and 1047053516597 (Esmeraldo-like haplotype) which were derived from the CL Brener chromosomal bands at 1.1 and 0.85 Mb, respectively. All of these microsatellite loci were mapped within inter-coding regions (untranslated or intergenic regions) and are therefore not associated with protein-coding sequences (Fig. 1).

There were not enough mapped markers for us to identify the correspondence between the chromosomal bands and the scaffolds containing the TcCAA10 locus. This locus was located on the scaffolds 1047053516799 (Esmeraldo-like haplotype) and 1047053516737 (non-Esmeraldo-like haplotype) within alleles of an uncharacterised gene (Tc00.1047053508385.20, Esmeraldo-like and Tc00.10470 53506791.20, non-Esmeraldo-like). Alignments between the DNA sequences of these two alleles showed a deletion of 33 nucleotides, which corresponds to the loss of nine (CAA) and two (CAG) repetitive units in the allele from the non-Esmeraldo-like haplotype. Thus, these alleles probably code two hypothetical proteins with different numbers of amino acids.

To establish a correlation between the sizes of the PCR amplified fragments and the DNA sequences obtained from the *T. cruzi* genome project (El-Sayed et al., 2005), the latter sequences were aligned with the 93.4 Kb contig from chromosome III (Andersson et al., 1998), which had been used to design the primers. The alignments revealed a high degree of identity among the DNA sequences analysed for all microsatellite loci with only punctual mutations, most of those within the non-Esmeraldo-like haplotype. We also observed a perfect relationship between the predicted allele size from DNA sequences obtained in the databases and those determined experimentally by PCR. For instance, by the time the primers for the TAC15 locus were designed, only a 129 bp amplicon containing 15 repetitive units was predicted for this locus within the 93.4 Kb contig from chromosome III. However after performing the PCR, in addition to this allele,

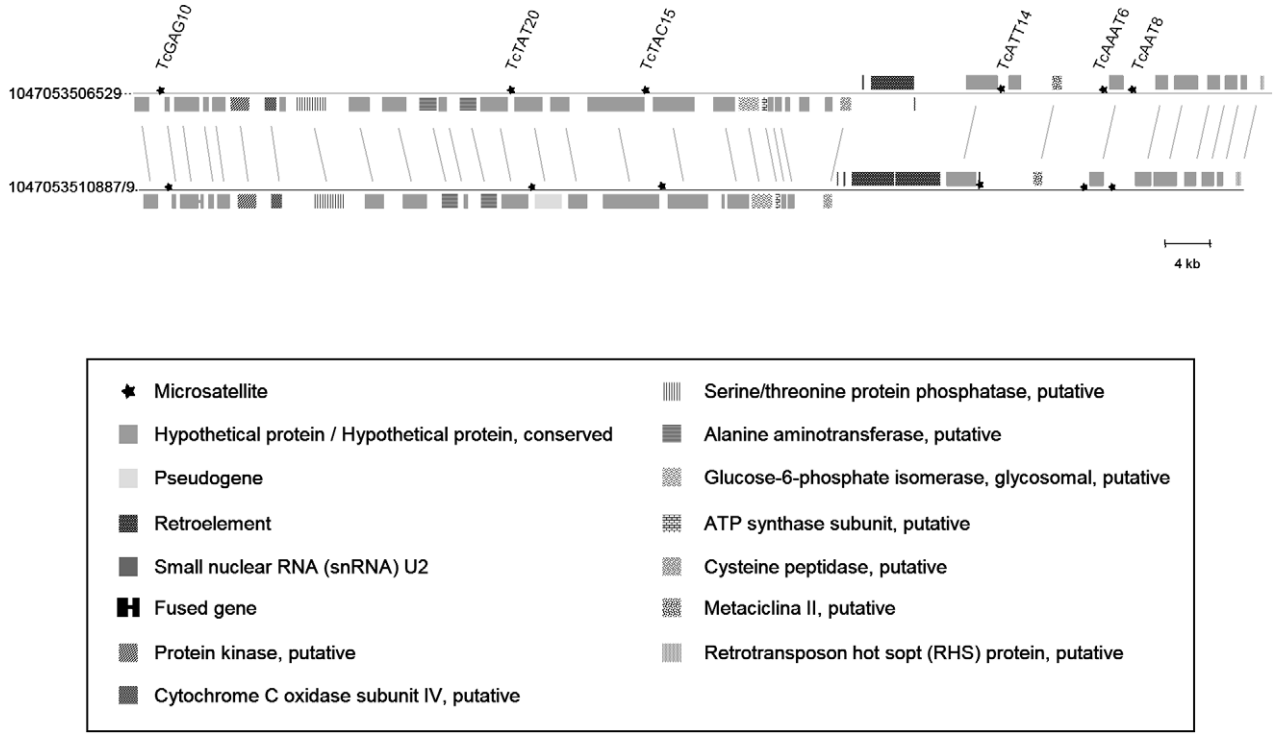

Fig. 1. Microsatellites in *Trypanosoma cruzi* chromosome III contigs. The microsatellite loci analysed in this study and mapped on *T. cruzi* chromosome III are shown together with the contig genes. The contig numbers are indicated on the left. Stars indicate the microsatellite loci. Genes shown above the line are oriented 5′ to 3′ left to right, whereas those shown below the line are in the reverse orientation. Alleles are linked by grey lines. The 1047053506529 contig corresponds to the Esmeraldo-like haplotype, whereas the 1047053510887 and 1047053510889 contigs correspond to the non-Esmeraldo-like haplotype.

another allele could be amplified which corresponds to a 141 bp fragment containing 19 repetitive units. In fact, further data from the genome project confirmed the existence of both alleles in the CL Brener clone (Fig. 2).

3.3. Mouse tissue analyses

To evaluate whether the designed microsatellite analyses were sensitive enough to profile *T. cruzi* directly in chronically infected tissues, we initially analysed hearts and recta of mice double-infected with JG and Col1.7G2 populations, and compared the microsatellite profiles with those previously obtained using the LSSP-PCR technique (Fig. 3). We observed a perfect correspondence between the parasite typing obtained by both techniques, although distinct microsatellite loci have presented different analytical sensitivities. TcAAAT6 proved to be the most sensitive microsatellite locus. The fluorescent analyses of TcAAAT6-amplified fragments in the automatic sequencer revealed that all hearts presented two alleles with 271 and 275 bp, characteristic of the JG strain, whilst the recta showed only one allele with 255 bp characteristic of the Col1.7G2 clone. Accordingly, analyses of TcTAC15, TcATT14 and TcGAG10 loci revealed amplicons in all hearts with 99, 265 and 141/144 bp, respectively, corresponding to the JG strain pattern, whilst the only two recta that presented amplification products showed fragments of 96, 253 and 144 bp, characteristic of the Col1.7G2 clone. For the remaining three microsatellite loci, we could only detect amplified products in hearts of the mice. Nevertheless, the hearts presented the alleles of 262, 190/217 and 143/146 bp, corresponding to the characteristic alleles of the JG strain for TcAAT8, TcTAT20 and TcCAA10 loci, respectively (Fig. 4). For all loci analysed, no PCR product

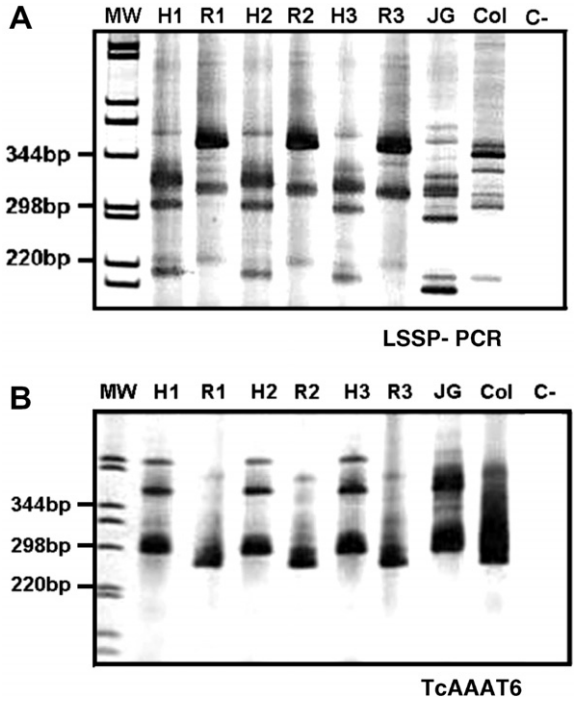

Fig. 3. Silver stained 6% polyacrylamide gel electrophoresis displaying infected mouse tissue amplicons obtained by low-stringency single-specific primer (LSSP)-PCR (A) and microsatellite locus TcAAAT6 analyses (B). MW, 1 Kb Ladder (Gibco-BRL); H, Heart; R, Rectum (numbers refer to mouse identification); JG, JG strain DNA; Col, Col1.7G2 clone DNA and C-, No DNA.

```
chromossome3      1 GGATATTTGTTACTGCTGGCGGTGGTGGTGGTGGCGGTGGGGCTGTGTACACAGCAATAT 60
1047053506529     1 GGATATTTGTTACTGCTGGCGGTGGTGGTGGTGGCGGTGGGGCTGTGTACACAGCAATAT 60
1047053510889     1 GGATATTTGTTACTGCTGGTGGTGGTGGTGGCGGTGGGGCTGTGTACACAGCAATAT 60
                                                    TcTAC15 Forward primer
chromossome3     61 TTGACCTTCTTTGTATTCTGACGGGGACAGGGCGAGAATTTCCCCATTTCCAAGCAAAGT 120
1047053506529    61 TTGACCTTCTTTGTATTCTGACGGGGACAGGGCGAGAATTTCCCCATTTCCAAGCAAAGT 120
1047053510889    61 TTGACTTTCTGTGGATTCTGACGGGGACAGGGCGAGAATTTCCC-ATTCCCAAGCAAAGT 119

chromossome3    121 AGGATAATCATATAAAAGAAATTACTACTACTACTACTACTACTACTACTACTACTA 180
1047053506529   121 AGGATAATCATATAAAAGAAATTACTACTACTACTACTACTACTACTACTACTACTA 180
1047053510889   120 AGGATAATCATATAAAAGAAATTACTACTACTACTACTACTACTACTACTACTACTA 179
                                                    TcTAC15 Reverse primer
chromossome3    181 CTACTACCA------------AAACAGAGGGACGCAGAAGCGATTGTTGCTCATCGCGTA 228
1047053506529   181 CTACTACCA------------AAACAGAGGGACGCAGAAGCGATTGTTGCTCATCGCGTA 228
1047053510889   180 CTACTACTACTACTACTACTAAAACAGAGGGACGCAGAAGCGATTGTTGCTCAACGCGTA 239

chromossome3    229 TACAACGAAGAAAAGAGTAATATATATATATATTTATTTATTTAAAAGAAGTTTCCATCA 288
1047053506529   229 TACAACGAAGAAAAGAGTAATATATATATATATTTATTTATTTAAAAGAAGTTTCCATCA 288
1047053510889   240 TACAACGAAGAGAAGAGTAATATATAT--------ATTTATTTAAAAGAAGGTTCCATCA 291

chromossome3    289 GGGGATTATCACCAATACGACTAGAGGGATATGTCCG 325
1047053506529   289 GGGGATTATCACCAATACGACTAGAGGGATATGTCCG 325
1047053510889   292 GGGGATTATCATCAATACGACTGGAGGGATATGTCCG 328
```

Fig. 2. TcTAC15 locus DNA sequence alignment. DNA sequences were obtained from a 93.4 Kb contig of *Trypanosoma cruzi* chromosome III and the DNA sequences from the *T. cruzi* genome project (1047053506529 and 1047053510889 scaffold numbers). These were aligned with Clustal W (1.83) multiple sequence alignment software (Higgins et al., 1994). Black shaded boxes indicate conserved nucleotides in all aligned DNA sequences. White boxes show nucleotides that are not conserved. Black bars over sequences represent the primer annealing sites.

was detected in the absence of DNA or in the presence of DNA from non-infected mouse tissues, demonstrating the high specificity of the PCR assays (data not shown).

3.4. Human tissue analyses

As well as the tissues of experimentally infected animals, we were able to detect *T. cruzi* microsatellite amplicons in different infected human tissues. We analysed nine different clinical samples including blood, CSF, heart, placenta and skin from infected patients. Five of those were amplified for all tested loci. Two samples were not amplified for the TcCAA10 locus and one was not amplified for the TcGAG10 locus. Due to insufficient DNA the Sk-L sample was only evaluated for three microsatellite loci (Table 4 and Fig. 5). Although TcAAT8 has shown to be the microsatellite locus with the greatest number of different alleles when amplified from DNA of parasites grown in vitro, it was excluded from the human tissues analyses because it presented low amplification efficiency in the full nested PCR strategy.

The 99 bp allele for the TcTAC15 locus was found in almost all analysed infected human tissues. It is interesting that the unique patient sample that has so far presented the allele of 96 bp corresponds to a CSF sample obtained from a patient presenting with Chagas encephalitis reactivation associated with AIDS, in which the infecting parasite was previously identified as belonging to the *T. cruzi* I lineage (AL in Table 4).

In two analysed cases (patients AS and HE) we detected three fragments of 99, 132 and 135 bp for the TcTAC15 locus, demonstrating a polyclonal constitution for the *T. cruzi* populations in the blood of these patients. This multiclonal structure was also observed in placental tissue from a *T. cruzi*-infected pregnant woman at the indeterminate phase of Chagas disease (PI). In this case, three fragments of 187, 190 and 220 bp were simultaneously amplified using the TcTAT20 locus (Table 4).

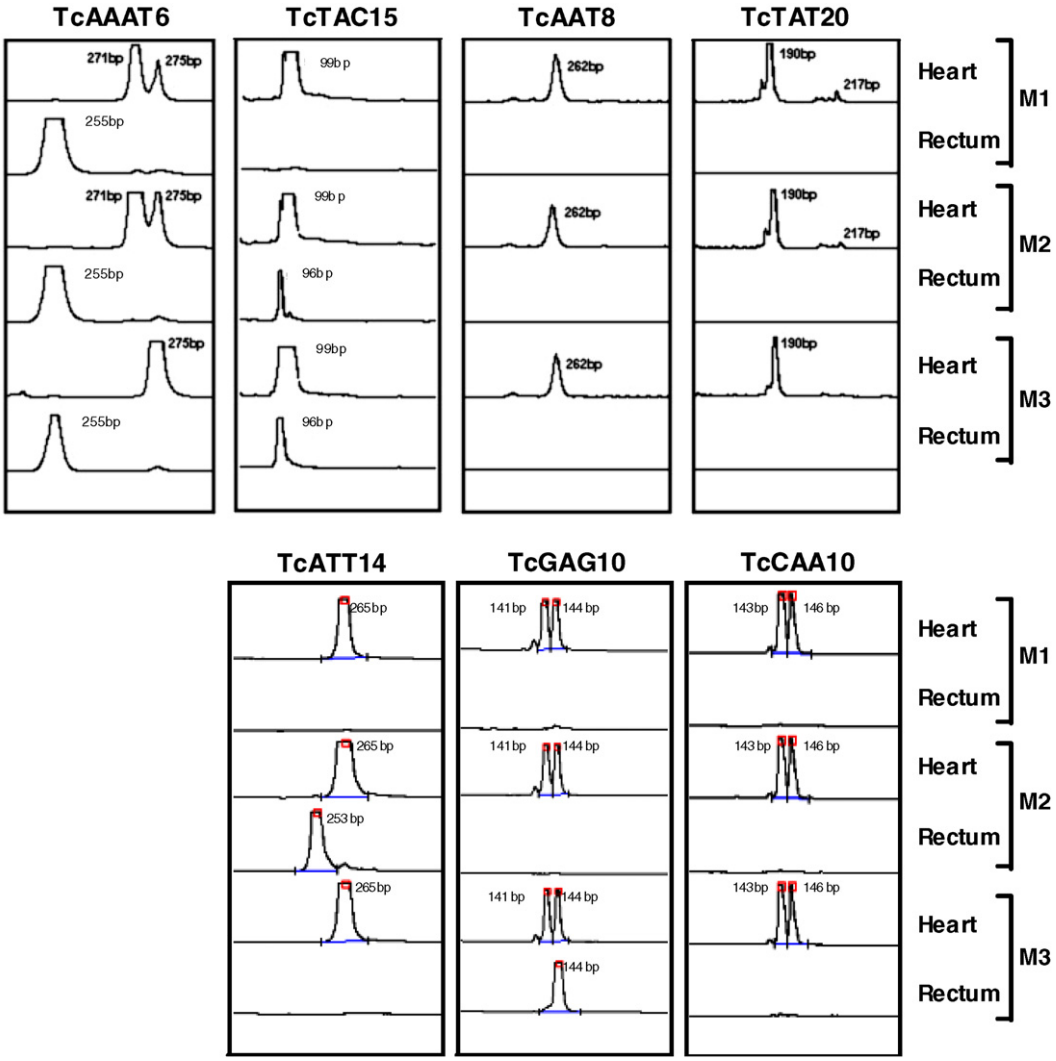

Fig. 4. Automatic laser fluorescent DNA sequencer electrofluorograms presenting the amplified fragments obtained by TcAAAT6, TcTAC15, TcAAT8, TcTAT20, TcATT14, TcGAG10 and TcCAA10 microsatellite loci analyses on infected mouse tissues. M1, Mouse 1, M2, Mouse 2 and M3, Mouse 3; numbers at the peaks refer to the size of the amplicons.

Table 4
Alleles sizes in bp obtained for each of the six loci analysed in nine different clinical samples of humans infected with *Trypanosoma cruzi*

Loci	TcAAAT6	TcTAT20	TcTAC15	TcATT14	TcGAG10	TcCAA10	Lineages[a]
Samples							
AL (CSF)	255/255	184/184	96/96	253/262	141/141	N.A.[b]	*T. cruzi* I
AS (blood)	255/255	184/220	99/132/135	253/265	144/144	N.A.[b]	Hybrid
HE (blood)	259/259	184/220	99/132/135	265/274	144/144	152/152	Hybrid
ChHD-T (blood)	255/255	181/181	129/129	262/262	N.A.[b]	149/149	Hybrid
ChHD-S (blood)	263/263	184/220	99/135	265/274	138/138	152/152	Hybrid
PI (placenta)	263/263	187/190/220	99/135	265/265	138/144	152/152	Hybrid
JP (heart)	263/275	199/211	99/99	262/262	144/144	155/155	*T. cruzi* II
DF (heart)	263/263	211/214	99/99	262/262	141/144	143/155	*T. cruzi* II
Sk-L (skin)	N.E.[c]	181/181	99/99	265/265	N.E.[c]	N.E.[c]	*T. cruzi* II

[a] The lineage of *T. cruzi* populations was previously determined by amplification of spliced leader gene intergenic regions (Burgos et al., 2007), the rDNA24Sα gene (Freitas et al., 2005) and citocrome oxidase II AluI restriction fragment length polymorphism (Freitas et al., 2006).
[b] N.A., not amplified by PCR.
[c] N.E., not evaluated.

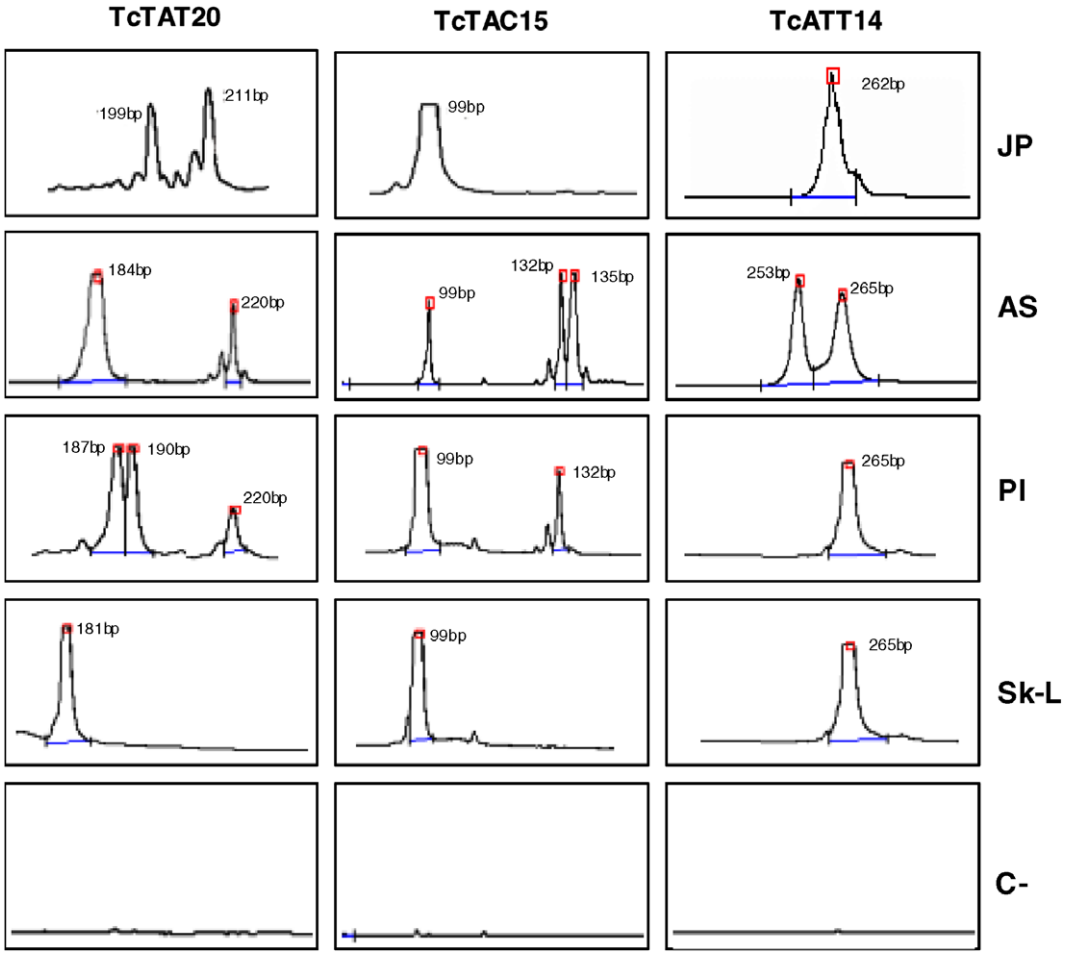

Fig. 5. Representative automatic laser fluorescent DNA sequencer electrofluorograms presenting the amplified fragments obtained by TcTAT20, TcTAC15 and TcATT14 microsatellite loci analyses of infected human tissues. JP, AS, PI and Sk-L correspond, respectively, to DNA obtained from heart, blood, placenta and skin of Chagasic patients. Numbers at the peaks refer to the size of the amplicons. (C) Represents the negative control (non-chagasic human DNA).

4. Discussion

In light of the Clonal Histotropic Model for the pathogenesis of Chagas disease (Macedo and Pena, 1998) we can assume that a powerful correlation between the parasite genetic and clinical aspects of the disease will only be demonstrated with direct profiling of *T. cruzi* populations present in tissue lesions. Nevertheless, the methods thus far described either were not sensitive enough to discriminate individual parasites directly from infected tissues or

generated very complex patterns that were difficult to interpret. Herein, based on a full nested PCR strategy designed to amplify microsatellite loci, we were able to detect and to evaluate genetic diversity of *T. cruzi* directly from infected animal and human tissues.

The seven new microsatellite loci (TcAAT8, TcTAT20, TcTAC15, TcATT14, TcGAG10, TcCAA10 and TcAAAT6) presented high levels of polymorphism, Hardy Weinberg departures and linkage disequillibrium comparable with those identified previously (Oliveira et al., 1998). These characteristics have been understood as evidence of a predominant clonal evolution and rare sexual reproduction for *T. cruzi* in which different lineages evolve independently of each other (Ayala, 1993; Tibayrenc, 1995). However, it has recently been clearly demonstrated that *T. cruzi* is capable of recombination in vitro (Gaunt et al., 2003) as well as under natural conditions (Machado and Ayala, 2001), but both the frequency and the mechanism of the sexual events remain to be determined. In this context, most of the microsatellite loci identified in this work are well distributed throughout a single chromosomal band, which renders them suitable for further investigations concerning recombination events in these parasites.

Exploring the data acquired from the whole-genome sequencing of the CL Brener clone, we could refine the localisation of the microsatellite loci, except for TcCAA10. All the other microsatellites were mapped on the chromosome III contigs together with four additional markers, including marker number 161, all of those belonging to linkage group I (Branche et al., 2006). The TcATT14, TcAAAT6 and TcAAT8 microsatellites were localised in proximity of each other, whereas TcTAC15, TcTAT20 and TcGAG10 were distributed across the contigs.

For all these loci, we were able to design two pairs of primers for full nested PCR assays. By using this strategy in experiments of serial dilutions of the *T. cruzi* DNA we could detect as little as 200 fentograms of DNA, which corresponds to the DNA content of a single parasite cell. This sensitivity, which is 100 to 1,000 times higher compared with conventional PCR, allowed us to detect specific *T. cruzi* amplicons in most of the tissue samples from infected mice. Despite the fact that the TcAAAT6, TcTAC15, TcATT14 and TcGAG10 loci detected parasite DNA in hearts and recta of all infected mice, the TcTAT20, TcAAT8 and the TcCAA10 loci were not able to detect the presence of *T. cruzi* DNA in the recta of the same animals. This could reflect a lower sensitivity of these three loci compared with the former, associated with a lower parasite burden in the recta than in the hearts of the animals. Furthermore, the microsatellite analyses permitted us to correctly identify the JG strain's homing for the hearts and Col1.7G2 for the recta of the mice, as previously demonstrated by means of the LSSP-PCR approach (Andrade et al., 1999).

The success of PCR directly in infected human tissues can be limited by diverse factors such as the small amount of parasites in the infected tissues and the varying reaction sensitivities of each microsatellite locus. Even taking into account these limitations with PCR, our main goal was to detect and characterise *T. cruzi* directly in these samples. Using the methodology described here we were able to amplify *T. cruzi* DNA directly in most of the infected human tissues analysed.

An interesting observation that emerges from the data presented here is the detection of the 99 bp alleles for the locus TcTAC15 in the majority of the analysed infected human tissues including blood, heart, placenta and a biopsy from a skin chagoma. Freitas et al. (2005) showed that only the rDNA 24Sα allele, typical of *T. cruzi* II strains, was found in chronically infected tissue samples from Brazilian patients. Similarly, based on the present data, it is reasonable to associate the amplification of the 99 bp allele for the TcTAC15 locus with parasite populations belonging to the major lineages *T. cruzi* II, III and hybrids, but not with *T. cruzi* I strains, which thus far have not presented the 99 bp allele. Nevertheless, the CSF sample collected from the patient AS, who presented with an episode of Chagasic encephalytis associated with AIDS, showed the TcTAC15 96 bp alleles, typical of *T. cruzi* I strains. This finding corroborates previous data that have demonstrated the *T. cruzi* I lineage causing human Chagas disease, ranging from asymptomatic to fatal cases in the northern part of South America (Coura et al., 2002; Añez et al., 2004; Teixeira et al., 2006).

Another important finding was the observation that patient AS was infected with a multiclonal bloodstream parasite population as revealed by the presence of three peaks (99, 132 and 135 bp alleles) in the TcTAC15 profile obtained from his blood sample, whereas a CSF sample collected from the same patient at the same time only depicted the TcTAC15 96 bp alleles. This confirms that microsatellite analyses constitute simple screening tests to evaluate whether *T. cruzi* stocks are monoclonal or multiclonal populations (Oliveira et al., 1998, 1999; Macedo et al., 2001, 2004). It also reports a new case in which different parasite populations colonise different locations in an immunosuppressed patient, as was recently described in another case of *T. cruzi* and HIV co-infection (Burgos et al., 2005). A multiclonal population (187, 190 and 220 bp alleles) has also been detected in a portion of placental tissue from a woman with asymptomatic *T. cruzi* infection who delivered a non-infected newborn, which in this case was revealed by the TcTAT20 locus.

In conclusion, we have described seven new microsatellite loci that are useful for different *T. cruzi* analyses including investigations of mechanisms of genetic exchange events and characterisation of parasites directly in infected tissues. The application of this strategy to a broad range of biological samples would certainly help to clarify the putative association between specific parasite genotypes, differential tissue tropisms and clinical manifestations of Chagas disease.

Acknowledgements

This work was supported by PRONEX CNPq/FAP-EMIG, CAPES, WHO. We thank the medicine students, Laura Gomide, Aline V. Santana, Andrea F. Silveira and Henrique C. R. Galvão, for helping in the experiments, Neuza A. Rodrigues and Kátia B. Gonçalves for expert technical assistance and to Drs Hector Freilij, Mirta Diez and M. Elena Seidenstein for clinical diagnosis and follow-up of Argentinean Chagas disease patients. Partial support of PIP 5369 and PICT 33955 to A.G.S.

References

Andersson, B., Aslund, L., Tammi, M., Tran, A.N., Hoheisel, J.D., Pettersson, U., 1998. Complete sequence of a 93.4-kb contig from chromosome 3 of *Trypanosoma cruzi* containing a strand-switch region. Genome Res. 8, 809–816.

Andrade, L.O., Machado, C.R., Chiari, E., Pena, S.D., Macedo, A.M., 1999. Differential tissue distribution of diverse clones of *Trypanosoma cruzi* in infected mice. Mol. Biochem. Parasitol. 100, 163–172.

Andrade, S.G., 1985. Morphological and behavioral characterization of *Trypanosoma cruzi* strains. Rev. Soc. Bras. Med. Trop. 18, 39–46.

Añez, N., Crisante, G., da Silva, F.M., Rojas, A., Carrasco, H., Umezawa, E.S., Stolf, A.M., Ramírez, J.L., Teixeira, M.M., 2004. Predominance of lineage I among *Trypanosoma cruzi* isolates from Venezuelan patients with different clinical profiles of acute Chagas' disease. Trop. Med. Int. Health 9 (12), 1319–1326.

Ayala, F.J., 1993. *Trypanosoma* and *Leishmania* have clonal population structures of epidemiological significance. Biol. Res. 26, 47–63.

Benson, G., 1999. Tandem Repeats Finder: a program to analyze DNA sequences. Nucleic Acids Res. 27, 573–580.

Branche, C., Ochaya, S., Aslund, L., Andersson, B., 2006. Comparative karyotyping as a tool for genome structure analysis of *Trypanosoma cruzi*. Mol. Biochem. Parasitol. 147, 30–38.

Brisse, S., Barnabé, C., Tibayrenc, M., 2000. Identification of six *Trypanosoma cruzi* phylogenetic lineages by random amplified polymorphic DNA and multilocus enzyme electroforesis. Int. J. Parasitol. 30, 34–44.

Brisse, S., Verhoef, J., Tibayrenc, M., 2001. Characterization of large and small subunit rRNA and mini-exon genes further supports the distinction of six *Trypanosoma cruzi* lineages. Int. J. Parasitol. 31, 1218–1226.

Burgos, J.M., Begher, S., Freitas, J.M., Bisio, M., Duffy, T., Altcheh, J., Teijeiro, R., Lopez Alcoba, H., Deccarlini, F., Freilij, H., Levin, M.J., Levalle, J., Macedo, A.M., Schijman, A.G., 2005. Molecular diagnosis and typing of *Trypanosoma cruzi* populations and lineages in cerebral Chagas disease in a patient with AIDS. Am. J. Trop. Med. Hyg. 73, 1016–1018.

Burgos, J.M., Altcheh, J., Bisio, M., Duffy, T., Valadares, H.M.S., Piccinali, R., Freitas, J.M., Levin, M.J., Macedo, A.M., Freilij, H., Schijman, A.G., 2007. Direct molecular profiling of minicircle signatures and lineages of *Trypanosoma cruzi* bloodstream populations causing congenital Chagas disease. Int. J. Parasitol. 37 (12), 1319–1327.

Coura, J.R., Junqueira, A.C., Fernandes, O., Valente, A.S., Miles, M.A., 2002. Emerging Chagas disease in Amazonian Brazil. Trends Parasitol. 18 (4), 171–176.

Di Noia, J.M., Buscaglia, C.A., De Marchi, C.R., Almeida, I.C., Frasch, A.C., 2002. A *Trypanosoma cruzi* small surface molecule provides the first immunological evidence that Chagas' disease is due to a single parasite lineage. J. Exp. Med. 185, 401–413.

El-Sayed, N.M., Myler, P.J., Bartholomeu, D.C., Nilsson, D., Aggarwal, G., Tran, A.N., Ghedin, E., Worthey, E.A., Delcher, A.L., Blandin, G., Westenberger, S.J., Caler, E., Cerqueira, G.C., Branche, C., Haas, B., Anupama, A., Arner, E., Aslund, L., Attipoe, P., Bontempi, E., Bringaud, F., Burton, P., Cadag, E., Campbell, D.A., Carrington, M., Crabtree, J., Darban, H., da Silveira, J.F., de Jong, P., Edwards, K., Englund, P.T., Fazelina, G., Feldblyum, T., Ferella, M., Frasch, A.C., Gull, K., Horn, D., Hou, L., Huang, Y., Kindlund, E., Klingbeil, M., Kluge, S., Koo, H., Lacerda, D., Levin, M.J., Lorenzi, H., Louie, T., Machado, C.R., McCulloch, R., McKenna, A., Mizuno, Y., Mottram, J.C., Nelson, S., Ochaya, S., Osoegawa, K., Pai, G., Parsons, M., Pentony, M., Pettersson, U., Pop, M., Ramirez, J.L., Rinta, J., Robertson, L., Salzberg, S.L., Sanchez, D.O., Seyler, A., Sharma, R., Shetty, J., Simpson, A.J., Sisk, E., Tammi, M.T., Tarleton, R., Teixeira, S., Van Aken, S., Vogt, C., Ward, P.N., Wickstead, B., Wortman, J., White, O., Fraser, C.M., Stuart, K.D., Andersson, B., 2005. The genome sequence of *Trypanosoma cruzi*, etiologic agent of Chagas disease. Science 309, 409–415.

Freitas, J.M., Augusto-Pinto, L., Pimenta, J.R., Bastos-Rodrigues, L., Goncalves, V.F., Teixeira, S.M., Chiari, E., Junqueira, A.C., Fernandes, O., Macedo, A.M., Machado, C.R., Pena, S.D., 2006. Ancestral genomes, Sex and the Population Structure of *Trypanosoma cruzi*. PLoS Pathogens 2, 226–235.

Freitas, J.M., Lages-Silva, E., Crema, E., Pena, S.D.J., Macedo, A.M., 2005. Real time PCR strategy for the identification of major lineages of *Trypanosoma cruzi* directly in chronically infected human tissues. Int. J. Parasitol. 35, 411–417.

Gaunt, M.W., Yeo, M., Frame, I.A., Stothard, J.R., Carrasco, H.J., Taylor, M.C., Mena, S.S., Veazey, P., Miles, G.A., Acosta, N., de Arias, A.R., Miles, M.A., 2003. Mechanism of genetic exchange in American trypanosomes. Nature 241, 936–939.

Higgins, D., Thompson, J., Gibson, T., Thompson, J.D., Higgins, D.G., Gibson, T.J., 1994. CLUSTAL W: improving the sensitivity of progressive multiple sequence alignment through sequence weighting, position-specific gap penalties and weight matrix choice. Nucleic Acids Res. 22, 4673–4680.

Hecker, K.H., Roux, K.H., 1996. High and low annealing temperatures increase both specificity and yield in touchdown and step-down PCR. Biotechniques 20, 478–485.

Macedo, A.M., Pena, S.D.J., 1998. Genetic variability of *Trypanosoma cruzi*: implication for the pathogenesis of Chagas' disease. Parasitol. Today 14, 119–123.

Macedo, A.M., Martins, M.S., Chiari, E., Pena, S.D., 1992. DNA fingerprinting of *Trypanosoma cruzi*: a new tool for characterization of strain and clones. Mol. Biochem. Parasitol. 55, 147–154.

Macedo, A.M., Pimenta, J.R., Aguiar, R.S., Melo, A.R., Chiari, E., Zingales, B., Pena, S.D.J., Oliveira, R.P., 2001. Usefulness of microsatellite typing in population genetic studies of *Trypanosoma cruzi*. Mem. Inst. Oswaldo Cruz 96, 407–413.

Macedo, A.M., Machado, C.R., Oliveira, R.P., Pena, S.D.J., 2004. *Trypanosoma cruzi*: genetic structure of populations and relevance of genetic variability to the pathogenesis of Chagas disease. Mem. Inst. Oswaldo Cruz 99, 1–12.

Machado, C.A., Ayala, F.J., 2001. Nucleotide sequences provide evidence of genetic exchange among distantly related lineages of *Trypanosoma cruzi*. Proc. Natl. Acad. Sci. USA 98, 7396–7401.

Melo, R.C., Brener, Z., 1978. Tissue tropism of different *Trypanosoma cruzi* strains. J. Parasitol. 64, 475–482.

Miles, M.A., Souza, A., Povoa, M., Shaw, J.J., Lainson, R., Toye, P.J., 1978. Isozymic heterogeneity of *Trypanosoma cruzi* in the first autochthonous patients with Chagas' disease in Amazoniam Brazil. Nature 272, 819–821.

Momen, H., 1999. Taxonomy of *Trypanosoma cruzi*: a commentary on characterization and nomenclature. Mem. Inst. Oswaldo Cruz 94, 181–184.

Morel, C., Chiari, E., Camargo, E.P., Mattei, D.M., Romanha, A.J., Simpson, L., 1980. Strain and clones of *Trypanosoma cruzi* can be characterized by patterns of restriction endonuclease products of kinetoplast DNA minicircles. Proc. Natl. Acad. Sci. USA 77, 6810–6814.

Oliveira, R.P., Broude, N.E., Macedo, A.M., Cantor, C.R., Smith, C.L., Pena, S.D., 1998. Probing the genetic population structure of *Trypanosoma cruzi* with polymorphic microsatellites. Proc. Natl. Acad. Sci. USA 95, 3376–3780.

Oliveira, R.P., Melo, A.I.R., Macedo, A.M., Chiari, E., Pena, S.D.J., 1999. The population structure of *Trypanosoma cruzi*: expanded analysis of 54 strains using eight polymorphic CA-repeat microsatellites. Mem. Inst. Oswaldo Cruz 94, 65–70.

Romanha, A.J., Pereira da Silva, A.A., Chiari, E., Kilgour, V., 1979. Isoenzyme patterns of cultured *Trypanosoma cruzi*: changes after prolonged subculture. Comp. Biochem. Physiol. 62B, 139–142.

Rychlick, W., 1992. OLIGO version 4.0. National Biosciences, Plymouth, Minnesota.

Schijman, A., Vigliano, C., Burgos, J.M., Favaloro, R., Perrone, S., Laguens, R., Levin, M.J., 2000. Early diagnosis of recurrence of *T. cruzi* infection by polymerase chain reaction after heart transplantation of a chronic Chagas' heart disease patient. J. Heart Lung Transplant. 19, 1114–1117.

Souto, R.P., Fernandes, O., Macedo, A.M., Campbell, D.A., Zingales, B., 1996. DNA markers define two major phylogenetic lineages of *Trypanosoma cruzi*. Mol. Biochem. Parasitol. 83, 141–152.

Teixeira, M.M.G., daSilva, F.M., Marcili, A., Umezawa, E.S., Shikanai-Yasuda, M.A., Cunha-Neto, E., Kalil, J., Stolf, N., Stolf, A.M., 2006. *Trypanosoma cruzi* lineage I in endomyocardail biopsy from a northeastern Brazilian patient at end-stage chronic chagasic cardiomyopathy. Trop. Med. Int. Health 11 (3), 294–298.

Tibayrenc, M., Ward, P., Moya, A., Ayala, F.J., 1986. Natural populations of *Trypanosoma cruzi*, the agent of Chagas' Disease, have a complex multiclonal structure. Proc. Natl. Acad. Sci. USA 83, 1335–1339.

Tibayrenc, M., 1995. Population genetics of parasitic protozoa and other microorganisms. Adv. Parasitol. 36, 47–115.

Vago, A.R., Andrade, L.O., Leite, A.A., d'Avila Reis, D., Macedo, A.M., Adad, S.J., Tostes Jr., S., Moreira, M.C., Filho, G.B., Pena, S.D.J., 2000. Genetic characterization of *Trypanosoma cruzi* directly from tissues of patients with chronic Chagas disease: differential distribution of genetic types into diverse organs. Am. J. Pathol. 156, 1805–1809.

Veas, F., Breniere, S.F., Cuny, G., Brengues, C., Solari, A., Tibayrenc, M., 1991. General procedure to construct highly specific kDNA probes for clones of *Trypanosoma cruzi* for sensitive detection by polymerase chain reaction. Cell Mol. Biol. 37 (1), 73–84.

Virreira, M., Serrano, G., Maldonado, L., Svoboda, M., 2006. *Trypanosoma cruzi*: typing of genotype (sub) lineages in megacolon samples from bolivian patients. Acta Trop. 100 (3), 252–255.

Zingales, B., Souto, R.P., Mangia, R.H., Lisboa, C.V., Campbell, D.A., Coura, J.R., Jansen, A., Fernandes, O., 1998. Molecular epidemiology of American trypanosomiasis in Brazil based on dimorphisms of rRNA and mini-exon gene sequences. Int. J. Parasitol. 28, 105–112.

Zingales, B., Stolf, B.S., Souto, R.P., Fernandes, O., Briones, M.R., 1999. Epidemiology, biochemistry and evolution of *Trypanosoma cruzi* lineages based on ribosomal RNA sequences. Mem. Inst. Oswaldo Cruz 94, 159–164.